Field-induced periodic distortions in a nematic liquid crystal: Deuterium NMR study and theoretical analysis

A. Sugimura*
Department of Information Systems Engineering, Osaka Sangyo University, 3-1-1 Nakagaito, Daito-shi, Osaka 574-8530, Japan

A. V. Zakharov†
Saint Petersburg Institute for Machine Sciences, The Russian Academy of Sciences, Saint Petersburg 199178, Russia
(Received 3 February 2011; revised manuscript received 22 April 2011; published 5 August 2011)

The peculiarities in the dynamic of the director reorientation in a liquid crystal (LC) film under the influence of the electric **E** field directed at an angle α to the magnetic **B** field have been investigated both experimentally and theoretically. Time-resolved deuterium NMR spectroscopy is employed to investigate the field-induced director dynamics. Analysis of the experimental results, based on the predictions of hydrodynamic theory including both the director motion and fluid flow, provides an evidence for the appearance of the spatially periodic patterns in 4-n-pentyl-4′-cyanobiphenyl LC film, at the angles $\alpha > 60^\circ$, in response to the suddenly applied **E**. These periodic distortions produce a lower effective rotational viscosity. This gives a faster response of the director rotation than for a uniform mode, as observed in our NMR experiment.

DOI: 10.1103/PhysRevE.84.021703 PACS number(s): 61.30.Cz, 65.40.De

I. INTRODUCTION

It is important, both from an academic and a technological point of view, to investigate the dynamic director reorientation in a thin nematic liquid crystal (NLC) film confined between two transparent electrodes and subject to competing constraints. In the presence of external electric and magnetic fields, and surface anchoring in a nematic film, the motion of the director, $\hat{\mathbf{n}}(r,t)$, to its equilibrium orientation, $\hat{\mathbf{n}}_{eq}(r)$, across the LC film is governed by elastic, electric, magnetic, and viscous torques. Taking into account the fact that the optical properties of the nematic phase are especially sensitive to external constraints, there is considerable interest in the dynamic director distribution and relaxation in the interior and at the bounding surfaces of a nematic cell. If the director is perturbed, for instance, by means of an electric field, and then allowed to relax, these torques vanish when the director alignes at the equilibrium angle, $\theta_{eq}(r)$, with respect to the normal, $\hat{\mathbf{k}}$, to the cell surfaces (see Fig. 1). Nuclear magnetic resonance (NMR) spectroscopy is by now a well-established method for investigating orientational order and dynamic properties in thermotropic liquid crystalline phases [1]. Deuterium NMR spectra are quite simple and give site-specific information, being dominated by intramolecular interactions, that is, the quadrupolar interaction and the homonuclear ^{2}H-^{2}H, and heteronuclear ^{2}H-^{1}H dipolar interactions. Therefore, deuterium is at present the most employed nucleus for studying both the orientational ordering and the director dynamics in the LC phases.

Recently, the time-resolved deuterium NMR spectroscopic measurements of field-induced director reorientations have been performed [2–6]. Taking into account the fact that the quadrupolar splitting is related to the angle θ made by the director **n** with the magnetic field **B** (see Fig. 1), deuterium NMR spectroscopy is found to be a powerful method with which to investigate the dynamic director reorientation in nematic films. We have used the deuterium NMR spectroscopy to investigate the director dynamics of deuteriated 4-α,α-d_2-*pentyl*-4′-cyanobiphenyl(5CB-d_2) subject to both magnetic and electric fields in the nematic phase. This gives a unique reorientation pathway. A sequence of deuterium NMR spectra was acquired as a function of time, which can be used to explore the dynamic director reorientation. When the electric field is applied to the nematic film, the director moves from being parallel to the magnetic field to being at an angle α to the magnetic field (the turn-on process), with the relaxation time τ_{ON}, because $\Delta\tilde{\epsilon}$ and $\Delta\tilde{\chi}$ are both positive for 5CB. Here $\Delta\tilde{\epsilon}$ denotes the nematic dielectric anisotropy and $\Delta\tilde{\chi}$ is the anisotropy of the diamagnetic susceptibility of the nematic phase. After the electric field is switched off, the director relaxes back to being parallel to the magnetic field (the turn-off process), with the relaxation time τ_{OFF}. Deuterium NMR spectra were recorded during the turn-on and turn-off alignment processes as a function of time. Analysis of these results shows that $\tau_{ON}(\alpha)$ monotonically grows with the increase of angle α, up to the maximum value $\tau_{ON}(\max)$. With further growth of α, up to the right angle ($\alpha \sim \frac{\pi}{2}$), $\tau_{ON}(\alpha \sim \frac{\pi}{2})$ rapidly decreases with a few milliseconds, with respect to $\tau_{ON}(\max)$.

The main objective of the present article is to study the peculiarities observed during the dynamic process of the director reorientation in the LC film, under the influence of a large electric field directed perpendicular to the magnetic field. This may cause an appearance of stripes in the sample. Physically, this means that a periodic distortion emerges spontaneously from the homogeneous state. It may induce a faster response than in the uniform mode, because it has a lower effective viscosity. To support this view, we discuss the complete system of hydrodynamic equations that includes both director reorientation and velocity field [7].

The outline of this paper is as follows. In the next section we describe the NMR experiment and the results obtained.

*sugimura@ise.osaka-sandai.ac.jp
†Author to whom correspondence should be addressed: avz0911@yahoo.com; www.ipme.ru

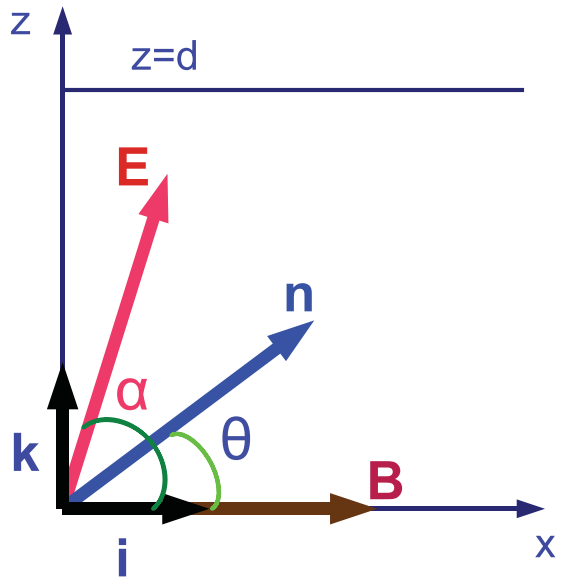

FIG. 1. (Color online) The geometry used for the calculations. The z axis is normal to the electrodes. The magnetic field **B**, electric field **E**, and director $\hat{\mathbf{n}}$, are in the xz plane. The director makes an angle θ both with the x axis and the magnetic field **B**, and the electric field makes an angle α with the magnetic field.

The theoretical treatment, including both the director motion and fluid flow in the nematic film and the numerical results for a number of hydrodynamical regimes, is given in Sec. III. The discussion of these results and our conclusions are summarized in Sec. IV.

II. DEUTERIUM NMR MEASUREMENT AND EXPERIMENTAL RESULTS

Deuterium NMR provides a powerful technique with which to investigate the director orientation in a liquid crystal [4], and we now describe briefly the background to this. The nuclear spin of deuterium is 1, so it possesses a quadrupole moment, which interacts with the electric field gradient at the nucleus to give a tensorial quadrupolar interaction. This does not influence the number of lines in the deuterium NMR spectrum for an isotropic liquid because the random and rapid molecular motion averages the quadrupolar interaction in the static spin Hamiltonian to zero. The NMR spectrum for a single deuteron, therefore, contains a single line composed of two degenerate spin transitions. In a LC phase the molecular rotation is no longer random, so the total quadrupolar tensor is not averaged to zero. In consequence the transitional degeneracy observed for the isotropic phase is removed. The deuterium NMR spectrum originating from a group of equivalent deuterons, with negligible dipolar interactions, for a nematic in which the director is parallel to the magnetic field consists of a doublet whose separation, the quadrupolar splitting, is denoted by $\Delta\tilde{\nu}_0$. This quadrupolar splitting is given, in a uniaxial phase, by [8]

$$\Delta\tilde{\nu}_0 = \tfrac{3}{2} q_{\mathrm{CD}} S_{\mathrm{CD}}, \tag{1}$$

where q_{CD} is the deuterium quadrupolar coupling constant and S_{CD} is the orientational order parameter of the C—D bond. This result is valid provided the quadrupolar tensor is taken to be uniaxial about the C—D bond, which is a reasonable approximation. When a sufficiently strong electric field is applied, the director tends to be aligned in the direction of the electric field provided the dielectric anisotropy is positive. Now, the dependence of the quadrupolar splitting, $\Delta\tilde{\nu}$, on the angle θ made by the director with the magnetic field of the NMR spectrometer is given by [9]

$$\Delta\tilde{\nu}(\theta) = \Delta\tilde{\nu}_0 P_2(\cos\theta), \tag{2}$$

where $\Delta\tilde{\nu}_0$ is the splitting when the director is parallel to the magnetic field and $P_2(\cos\theta)$ is the second Legendre polynomial. The form of this angular dependence results from the uniaxial symmetry of the motionally averaged quadrupolar tensor and does not depend on the symmetry of the total tensor or of the molecule. As the director moves from being parallel to the magnetic field the splitting is predicted, and observed, to decrease, pass through zero at the so-called magic angle ($\theta = 54.74^\circ$), and then to increase to one-half of $\Delta\tilde{\nu}_0$ when the director is orthogonal to the magnetic field. Strictly the quadrupolar splitting changes sign at the magic angle but the sign of the splitting is not directly available from the spectrum. This would create a difficulty when the splitting is less than or equal to one-half of $\Delta\tilde{\nu}_0$; for example, if $|\Delta\tilde{\nu}_0(\theta)/\Delta\tilde{\nu}_0|$ was exactly $1/2$ then the angle could be either 38.26° or 90°. Fortunately, this is not a problem in our experiments, for as we shall see the quadrupolar splitting varies continuously from $\Delta\tilde{\nu}_0$ so its sign, or rather its relative sign, is not in doubt. Thus, the value of the angle θ can be determined directly from Eq. (2) by measuring the quadrupolar splittings, $\Delta\tilde{\nu}(\theta)$ and $\Delta\tilde{\nu}_0$.

The essential feature of our experimental study is to vary the director orientation with respect to the magnetic field with the aid of an electric field applied across a thin nematic slab. By varying the strength of the electric field, the total balance of both the magnetic and electric fields, the surface torque, and the elastic torque can be controlled. To see how the factors determine the director orientation in the presence of the two fields we consider a monodomain sample and ignore surface anchoring effects, which is a reasonable assumption for a thick cell ($\sim$200 μm) with untreated electrode surfaces. Since the director is uniformly aligned we can also ignore the elastic energy. The geometry for this system is shown in Fig. 1, where the electric field makes an angle α with the magnetic field. The director orientation is obtained from the torque-balance equation which for a monodomain nematic is

$$\frac{\Delta\tilde{\chi}}{2\mu_0} B^2[\sin 2\theta - \rho \sin 2(\alpha - \theta)] = 0, \tag{3}$$

where

$$\rho = \frac{U_{\mathrm{E}}}{U_{\mathrm{M}}} = \epsilon_0\mu_0 \frac{\Delta\tilde{\epsilon}}{\Delta\tilde{\chi}} \left(\frac{E}{B}\right)^2, U_{\mathrm{M}} = \frac{\Delta\tilde{\chi}}{2\mu_0} B^2, U_{\mathrm{E}} = \frac{\epsilon_0 \Delta\tilde{\epsilon}}{2} E^2, \tag{4}$$

μ_0 is the magnetic permeability, and ϵ_0 the dielectric permittivity of a vacuum. The parameter ρ is the ratio of the anisotropic magnetic, U_{M}, and electric, U_{E}, energies. That is, $\rho = 1$ means that the two anisotropic field energies are

equal. The equilibrium value of the director orientation, θ_∞, sometimes called the limiting angle, is given by [2]

$$\cos 2\theta_\infty = \frac{1+\rho\cos 2\alpha}{\sqrt{1+2\rho\cos 2\alpha+\rho^2}}. \tag{5}$$

The director orientation depends, therefore, on the material property, $\Delta\tilde{\epsilon}/\Delta\tilde{\chi}$, and the known experimental parameters E/B and α. It is clear from Eq. (5) that the equilibrium angle is not exactly the same as the angle between the two fields because the values of ρ used in the experiment are insufficient to align the director parallel to the electric field.

As we have seen, the angle α between the electric and magnetic fields is one of the important experimental parameters needed to investigate the director orientation. However, it is difficult to determine this angle precisely because the electric field strength used in our measurements is not quite high enough to align the director parallel to the electric field. As reported previously [2], Eqs. (2) and (5) show that the quadrupolar splitting ratio for a certain applied voltage V gives the limiting angle θ_∞. This was achieved by rearranging Eq. (5) and combining it with Eq. (2) to give [3]

$$q(\Delta\tilde{\nu}/\Delta\tilde{\nu}_0) = \frac{1}{a\sin 2\alpha}\frac{1}{V^2} + \cot 2\alpha, \tag{6}$$

where

$$g(\Delta\tilde{\nu}/\Delta\tilde{\nu}_0) = \frac{4(\Delta\tilde{\nu}/\Delta\tilde{\nu}_0)-1}{2\sqrt{[2-2(\Delta\tilde{\nu}/\Delta\tilde{\nu}_0)][1+2(\Delta\tilde{\nu}/\Delta\tilde{\nu}_0)]}},$$
$$a = \frac{\mu_0\epsilon_0}{B^2d^2}\frac{\Delta\tilde{\epsilon}}{\Delta\tilde{\chi}}, \tag{7}$$

and d is the cell thickness. The function $g(\Delta\tilde{\nu}/\Delta\tilde{\nu}_0)$ is seen to be linear in $1/V^2$; accordingly, α and a, that is, $\Delta\tilde{\epsilon}/\Delta\tilde{\chi}$, can be found from a linear least-squares fit of the experimental NMR data for the voltage dependence of the quadrupolar splittings to Eqs. (6) and (7).

When an electric field of sufficient strength is applied to the nematic film, the director moves from being parallel to the magnetic field to being at an angle with respect to it (the turn-on process) because $\Delta\tilde{\epsilon}$ and $\Delta\tilde{\chi}$ are both positive for 5CB used in our experiments. After the electric field is switched off, the director relaxes back to being parallel to the magnetic field (the turn-off process). Time-resolved deuterium NMR spectra recorded during the turn-on and the turn-off alignment processes can be analyzed in terms of the Leslie-Ericksen theory to give the field-induced director relaxation times. In the dynamic analysis, we also treat the director as being uniformly aligned and use the quadrupolar splitting measured for this doublet to calculate the angle between the director and the magnetic field. The rate of change of the director orientation is given, for the turn-on process, by the torque-balance equation [10,11] which for a monodomain nematic [12] is

$$\gamma_1\frac{d\theta(t)}{dt} = -\frac{\Delta\tilde{\chi}}{2\mu_0}B^2\{\sin 2\theta(t) - \rho\sin 2[\alpha-\theta(t)]\}, \tag{8}$$

where γ_1 is the rotational viscosity coefficient. The solution of Eq. (8) is obtained analytically as [12]

$$\theta(t) = \theta_\infty + \tan^{-1}\left[\tan(\theta_0-\theta_\infty)\exp\left(-\frac{t}{\tau}\right)\right], \tag{9}$$

where θ_∞ is the limiting value of $\theta(t)$ when t tends to infinity, τ is the relaxation time for the director rotation, and θ_0 is the initial angle. The relaxation times for the turn-on (τ_{ON}) and turn-off (τ_{OFF}) processes are then

$$\tau_{ON} = \frac{1}{\sqrt{\tau_M^{-2}+2\tau_M^{-1}\tau_E^{-1}\cos 2\alpha+\tau_E^{-2}}} = \frac{\tau_M}{\sqrt{1+2\rho\cos 2\alpha+\rho^2}} \tag{10}$$

and

$$\tau_{OFF}(\equiv\tau_M) = \frac{\gamma_1}{2U_M}, \tag{11}$$

$$\tau_E = \frac{\gamma_1}{2U_E}, \tag{12}$$

respectively, and τ_E and τ_M are the electric and magnetic field-induced relaxation times for the director, respectively. Equations (5) through (12) give the following simple relationships:

$$\sin^2 2\alpha = \frac{R^2\sin^2 2\theta_\infty}{R^2-2R\cos 2\theta_\infty+1}, \tag{13}$$

where

$$R = \frac{\tau_{OFF}}{\tau_{ON}} = \sqrt{\rho^2+2\rho\cos 2\theta_\infty+1}. \tag{14}$$

It is evident from Eqs. (13) and (14) that α can be determined using θ_∞ measured from the quadrupolar splitting. We can see from Eq. (5) that the static experiments give ρ from which the material property $\Delta\tilde{\epsilon}/\Delta\tilde{\chi}$ can be determined. It is also evident from Eqs. (10) through (12) that the dynamic experiments provide the two pure relaxation times, τ_E and τ_M, for the alignment of the director by electric and magnetic fields, respectively. Since the field strengths are known, the relaxation times are related to the material properties $\gamma_1/\Delta\tilde{\epsilon}$ and $\gamma_1/\Delta\tilde{\chi}$, respectively. The ratio of these is just $\Delta\tilde{\epsilon}/\Delta\tilde{\chi}$, which permits a check with the static experiments. To obtain the rotational viscosity coefficient it is necessary to know $\Delta\tilde{\chi}$ or $\Delta\tilde{\epsilon}$ from separate experiments. In practice it proves to be easier to determine accurate values for $\Delta\tilde{\epsilon}$ than for $\Delta\tilde{\chi}$. The static and dynamic NMR experiments then lead to the physical properties of the nematic phase.

The nematogen used for our study was pentylcyanobiphenyl (5CB-d_2), which had been specifically deuteriated in the α position of the pentyl chain. The diamagnetic anisotropy and the dielectric anisotropy of 5CB are both positive. A thin nematic sandwich cell ($d = 194.7$ μm thick) was prepared. The glass plates were coated with transparent In_2O_3 to act as electrodes. Since the transparent electrodes were not treated in any way, these surfaces give a weak anchoring at the interface with 5CB-d_2. The cell was held together by a special glue that is stable in the presence of the cyanobiphenyls and can be cured using UV radiation for a few minutes. All of the measurements were made at a constant temperature of 15 °C in the nematic phase of 5CB-d_2. The spectra were recorded using a JEOL Lambda 300 spectrometer, which has a magnetic flux density, B, of 7.05 T. The spectra were obtained using a quadrupolar echo sequence, with a 90° pulse of 7.7 μs and an interpulse delay of 40 μs. The repetition rate was 0.3 s. The number of free induction decays (FID's)

used to produce spectra with good signal to noise varied from 2000 to 20 000 depending on the sharpness of the spectral lines observed during the alignment process. The nematic cell was held in the NMR probe head so that the electric field, whose direction is normal to the substrate surface, makes an angle, α, with the magnetic field (see Fig. 1). The final adjustment of the orientation of the cell, to ensure that the electric field makes the desired angle with the magnetic field, was carried out by switching on a high electric potential (200 V_{RMS}) and rotating the cell by a few degrees using an ultrasonic stepping motor until the appropriate quadrupolar splitting was obtained. An amplifier and a function generator were used to provide a 4-kHz sinusoidal ac electric field to the cell. This frequency is sufficient to overcome the effects of ionic conduction and to provide a time resolution of 0.25 ms during the turn-on and turn-off dynamics measurements. In addition, this frequency is sufficiently high that the director experiences an essentially constant electric field during the turn-on process as required in the standard hydrodynamic analysis [12]. On applying or removing the electric field, the director orientation is expected in a plane defined by **B** and **E**.

Static deuterium NMR spectra were measured as a function of the applied electric potential for several angles of α. An example of a set of the spectra recorded for $\alpha \approx 80^\circ$ is shown in Fig. 2. The voltage dependence of the spectra shows that with increasing electric field strength the quadrupolar splitting

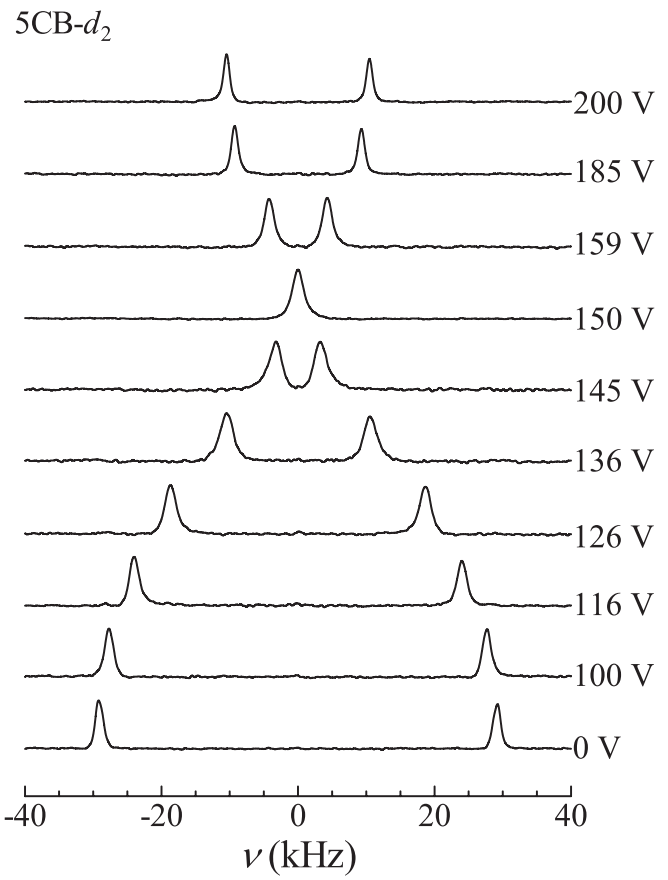

FIG. 2. Voltage dependence of the spectra recorded for $\alpha \approx 80^\circ$ at 15 °C.

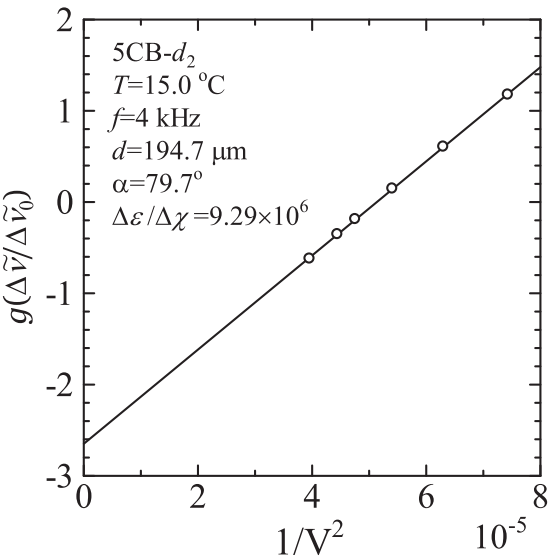

FIG. 3. Plot of $g(\Delta\nu/\Delta\nu_0)$ against $1/V^2$. Open circles show the experimental results using $\Delta\nu/\Delta\nu_0$ measured for various voltages. Solid line shows a least-squares fitting line using Eq. (6) to obtain the values of $\alpha = 79.7^\circ$ and $\Delta\epsilon/\Delta\chi = 8.28 \times 10^6$.

is reduced, passes through zero, and then increases again to less than half its original value. It would seem that the director orientation changes more or less continuously from being parallel to the magnetic field to being almost parallel to the electric field, as its strength grows. This change of the quadrupolar splitting follows Eq. (2). Those experimental data of the voltage dependence of $\Delta\tilde{\nu}/\Delta\tilde{\nu}_0$ were used to plot $g(\Delta\tilde{\nu}/\Delta\tilde{\nu}_0)$ against $1/V^2$ as shown in Fig. 3. Least-squares fitting of $\Delta\tilde{\nu}/\Delta\tilde{\nu}_0$ and V determines the values of $\alpha = 79.7^\circ$ and $\Delta\tilde{\epsilon}/\Delta\tilde{\chi} = 9.29 \times 10^6$ at 15 °C. Subsequently the static measurements of the deuterium NMR spectra as a function of voltage determine the values of α and $\Delta\tilde{\epsilon}/\Delta\tilde{\chi}$. These give the value of ρ and θ_∞ by using Eqs. (4) and (5), respectively.

Time-resolved NMR spectra were recorded during the turn-on and turn-off processes for various values of α determined by the static NMR measurements. For the turn-on and turn-off processes the director relaxation was monitored at several values following the application of the electric potential (200 V_{RMS}) and removal. A set of the NMR spectra recorded during the turn-on and turn-off processes for $\alpha = 79.7^\circ$ are shown in Figs. 4(a) and 4(b), respectively, as an example. In the turn-on process, the quadrupolar splitting decreases and then saturates with time after about 10 ms. In the turn-off process, the quadrupolar splitting increases because the director moves from being at $\theta = 71.9^\circ$ to the magnetic field to being parallel to it. The recorded spectra in the fast time region for the turn-on and turn-off processes contain weak oscillatory spectral features associated with the director rotation during the acquisition time for the FID. The origin of the oscillatory spectral features is understood [13], but they are not of importance for this investigation. The time dependence of the director orientation can be easily determined from our experimental results contained in the quadrupolar doublets because of the simple relation between the quadrupolar splitting and the director orientation described in Eq. (2).

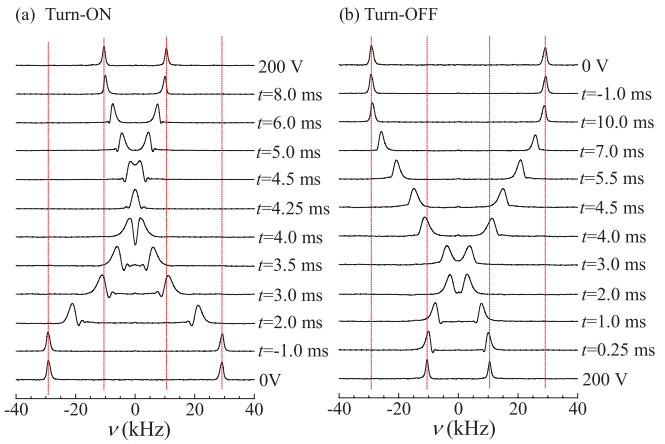

FIG. 4. (Color online) The deuterium NMR spectra of 5CB-d_2 for the (a) turn-on and (b) turn-off processes recorded at 15 °C under the condition of $\alpha = 79.7^\circ$ after the application of pulsed voltage (4 kHz, 200 V_{RMS}).

If we neglect the director distribution that causes the slight broadening of the spectral lines, then an appropriate form of the time dependence of the director orientation can be determined relatively easily. This is a good assumption since there is no elastic deformation in the nematic slab used in our experiments.

The time-resolved deuterium NMR spectra give the temporal variation in the ratio of the quadrupolar splitting frequency, $\Delta\nu/\Delta\nu_0$. These ratios and Eq. (2) give the director orientation as a function of time during the turn-on and turn-off processes at each angle α as shown by the symbols in Figs. 5(a) and 5(b), respectively. We can see in Fig. 5(a) that for the turn-on process the director rotates from the initial angle $\theta_0 = 0^\circ$ and then aligns at the limiting angle θ_∞. In the turn-off process shown in Fig. 5(b), the director rotates back parallel to the magnetic field; the time taken for the alignment process is slower in the turn-off process than in the turn-on process. It is possible to evaluate the relaxation times τ_{ON} and τ_{OFF} at each angle α, which were obtained by fitting the $\Delta\nu/\Delta\nu_0$ as a function of time by using Eqs. (2) and (9)–(11). The solid lines in Figs. 5(a) and 5(b) show the best-fit lines giving the values of τ_{ON} and τ_{OFF}.

Figure 6 shows the angle, α, dependencies of the relaxation times, τ_{ON} and τ_{OFF}. The open and closed circles indicate τ_{ON} and τ_{OFF} obtained from the best fits in Figs. 5(a) and 5(b), respectively. The solid lines are calculated results for τ_{ON} and τ_{OFF} by using Eqs. (10) and (11), respectively. In the calculations the values $B = 7.05$ T, $d = 194.7\ \mu m$, $V = 200$ V, and $\rho = 2.20$ were used. Two necessary values are the diamagnetic anisotropy and the rotational viscosity. In order to obtain these values from our results, we need the value of $\Delta\tilde{\epsilon}$ at 15 °C. For this we have used the extrapolated value of $\Delta\tilde{\epsilon} = 11.5$ at 15 °C from the temperature dependence of the dielectric anisotropies reported in the literature [14]. Now the value of $\Delta\tilde{\chi} = 1.24 \times 10^{-6}$ can be obtained from $\Delta\tilde{\epsilon} = 11.5$ and $\Delta\tilde{\epsilon}/\Delta\tilde{\chi} = 9.29 \times 10^6$ determined by the static measurement. The relaxation time of $\tau_{OFF} = 2.80$ ms and $\Delta\tilde{\chi}$ give $\gamma_1 = 0.136$ Pa s at 15 °C. It is clearly apparent from Fig. 6 that the relaxation time τ_{OFF} for the turn-off process

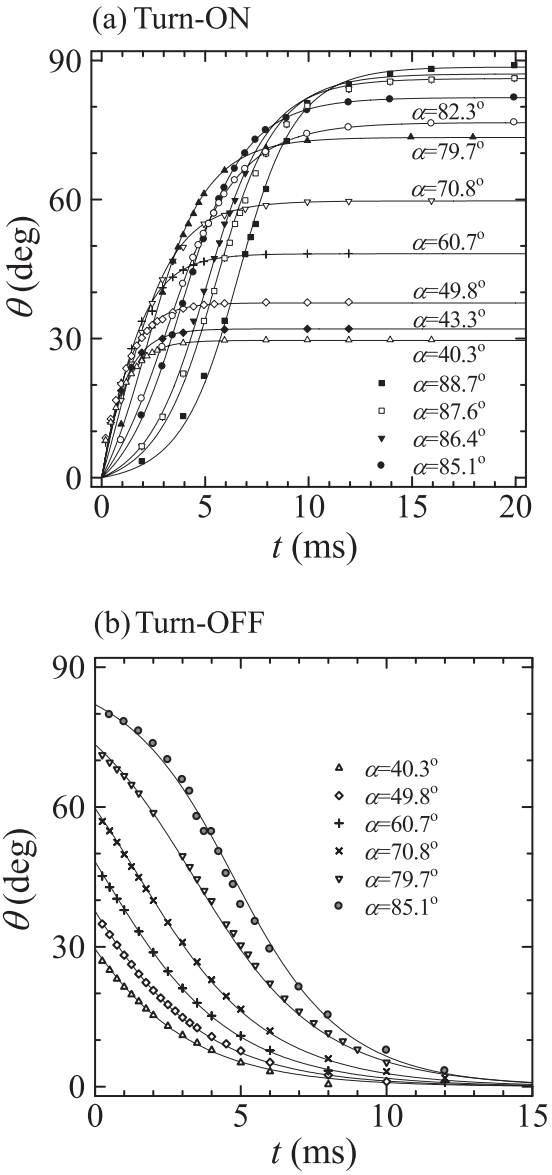

FIG. 5. (Color online) The time dependence of the director orientation for the turn-on (a) and the turn-off (b) processes at each angle α. The symbols were determined from the quadrupolar splitting ratio, $\Delta\tilde{\nu}/\Delta\tilde{\nu}_0$, with time. The solid lines show the best-fit lines giving the values of τ_{ON} and τ_{OFF} obtained by using Eqs. (2) and (9)–(11).

is independent of α, except for the condition of $\alpha \sim \frac{\pi}{2}$, and that τ_{ON} for the turn-on process depends on α. This dependence follows from the theory [see Eqs. (10) and (11)] for the monodomain director rotation when α is smaller than about 70°. It is also apparent that when α tends to be 90°, τ_{ON} is apart from the theoretical curve for the monodomain director rotation and starts to decrease. As described in Sec. II, the average director orientation with the magnetic field is estimated by the splitting frequency of the NMR spectral doublet. For larger α than about 80°, the spectral line shape recorded with time shows the broadening. This means that the director distributes around the average orientation. That is, the director distribution is no longer monodomain. At the moment we have no correct theoretical answer to the

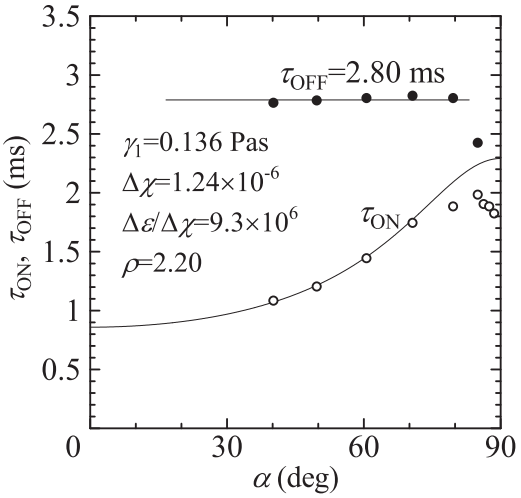

FIG. 6. The angle, α, dependencies of the relaxation times, τ_{ON} and τ_{OFF}. The open and closed circles indicate τ_{ON} and τ_{OFF} obtained from the best-fits in Fig. 5(a) and 5(b), respectively. The solid lines are calculated results for τ_{ON} and τ_{OFF} by using Eqs. (10) and (11), respectively.

director distribution, which may be produced by the periodic deformation of the director (see below). When α is larger than 89°, the NMR spectra recorded during the relaxation processes for turn-on and turn-off show the line broadening; for further increase of α close to 90° the spectra change to powderlike spectral line shapes. These would respond the spread of the director distribution. Since anomalous changes of the spectral line shapes do not give any information about the average director orientation, the experimental results discussed in this paper were limited in a region giving a uniform director orientation. Nonuniform director alignment is beyond the scope of the present subject and will be discussed elsewhere.

Such peculiarities observed during the director reorientation in the LC film subjected to strong electric field may be caused by the appearance of stripes in the LC sample in response to suddenly applied **E**. This gives a faster response to the director rotation than for a uniform mode, as observed in the experiment (see Fig. 6). In the next section, we will investigate the dynamics of the director reorientation in the LC film confined between two glass plates, based on the hydrodynamic theory including the director motion and fluid flow [10,11].

III. THEORETICAL TREATMENT AND CALCULATIONS

The essential feature of our theoretical investigation is to explore the director reorientation with respect to the magnetic field **B**, with the aid of the electric field **E** applied at the angle α to the magnetic field. By varying the strength of the electric field, total balance of the magnetic, electric, elastic, and viscous torques can be controlled. To see how the factors determine the director reorientation in presence of the magnetic and electric fields, when the angle α is close to a right angle, we consider initially homogeneously aligned liquid crystal film confined between two glass plates and with accounting for the surface anchoring effects. Notice that in our experiment the transparent electrodes were not treated in any way; these surfaces provide weak anchoring at the interface with 5CB-d_2. When strong electric field **E** is applied to the nematic film, the director moves from being parallel to the magnetic field to being parallel to the electric field **E**, with bend and splay deformations produced between the interior and aligned walls. When the angle α is close to a right angle, any small perturbation in the initially uniform alignment will begin to grow exponentially with a rate inversely proportional to some effective viscosity during the backflow reorientation process. Physically, this means that in the LC film, in response to the suddenly applied large electric field **E**, the spatially periodic strip patterns may appear. These periodic distortions are expected to give a faster response of the director reorientation than that for the monodomain mode [6,15–19] because it has a lower effective viscosity.

We try to understand the effects of a periodic pattern on the reorientation process. As seen in the experimental geometry, the director orientation is expected to be on the plane defined by **B** and **E**. Therefore, it is a good assumption that distortion has a small amplitude that will be modulated in the z direction (see Fig. 1), all physical quantities depend only on x and z) coordinates, and in the case of the planar geometry both the director $\hat{\mathbf{n}} = (n_x,0,n_z)$ and velocity $\mathbf{v} = (v_x,0,v_z)$ fields are in the xz plane. Assuming an incompressible fluid, the hydrodynamic equations describing the reorientation of the director can be derived from the balance of the elastic, viscous, magnetic, and electric torques $\mathbf{T}_{elast} + \mathbf{T}_{vis} + \mathbf{T}_{mag} + \mathbf{T}_{el} = 0$ and the Navier-Stokes equation for the velocity field **v**. For a system in which the inertial term is negligible the last equation takes the form

$$\partial_j p = \partial_i \sigma_{ij} \quad (i,j = x,z), \tag{15}$$

where the first term refers to the gradients of the pressure p and the second to the gradients of the viscous stress tensor σ_{ij} that are algebraic expressions of the director components and the velocity gradients [10,11]. In the case of the quasi-two-dimensional (2D) system the Navier-Stokes equation, Eq. (15), reduces to

$$\begin{aligned} p_{,x} &= \eta_5 v_{x,xx} + \eta_1 v_{x,zz} + \eta_4 v_{z,xz} + \alpha_3 n_{z,zt}, \\ p_{,z} &= \eta_2 v_{z,xx} + \eta_6 v_{x,xz} + 2\eta_3 v_{z,zz} + \alpha_2 n_{z,xt}, \end{aligned} \tag{16}$$

whereas the incompressibility condition $\nabla \cdot \mathbf{v} = 0$ reduces to

$$v_{x,x} + v_{z,z} = 0, \tag{17}$$

where $n_t = \partial n/\partial t$, $n_{z,zt} = \partial^2 n_z/\partial z \partial t$ and $p_{,x} = \partial p/\partial x$. Here $\eta_1 = \frac{1}{2}(\alpha_4 + \alpha_3 + \alpha_6)$, $\eta_2 = \frac{1}{2}(\alpha_4 + \alpha_5 - \alpha_2)$, $\eta_3 = \frac{1}{2}\alpha_4$, $\eta_4 = \frac{1}{2}(\alpha_4 + \alpha_6 - \alpha_3)$, $\eta_5 = \alpha_1 + \alpha_4 + \alpha_5 + \alpha_6$, $\eta_6 = \frac{1}{2}(\alpha_2 + \alpha_4 + \alpha_5)$, and α_i $(i = 1,\ldots,6)$ are the six temperature-dependent Leslie coefficients.

In the case of the linearized quasi-2D LC system, the torque balance equation composed of the elastic torque $\mathbf{T}_{elast} = -\hat{\mathbf{n}} \times \frac{\delta \mathcal{F}_{elast}}{\delta \hat{\mathbf{n}}} = [-K_1 n_{z,zz} - K_3 n_{z,xx}]\hat{\mathbf{j}}$, viscous torque $\mathbf{T}_{vis} = \hat{\mathbf{n}} \times (\gamma_1 \mathbf{N} + \gamma_2 \mathbf{A} \cdot \hat{\mathbf{n}}) = [\gamma_1 n_{z,t} + \alpha_2 v_{z,x} + \alpha_3 v_{x,z}]\hat{\mathbf{j}}$, magnetic torque $\mathbf{T}_{mag} = \frac{\Delta\tilde{\chi}}{\mu_0} B^2 n_z \hat{\mathbf{j}}$, and electric

$\mathbf{T}_{\rm el} = \epsilon_0 \Delta\tilde{\epsilon} E^2 \cos 2\alpha n_z \hat{\mathbf{j}}$ contributions can be written as

$$\gamma_1 n_{z,t} + \alpha_2 v_{z,x} + \alpha_3 v_{x,z} + \epsilon_0 \Delta\tilde{\epsilon} E^2 \cos 2\alpha n_z + \frac{\Delta\tilde{\chi}}{\mu_0} B^2 n_z - K_1 n_{z,zz} - K_3 n_{z,xx} = 0. \tag{18}$$

Here $\gamma_1 = \alpha_3 - \alpha_2$ and $\gamma_2 = \alpha_3 + \alpha_2$ are the rotational viscosity coefficients, and K_1 and K_3 are the splay and bend elastic constants.

The torque balance transmitted to the surfaces assumes that the director must satisfy the boundary conditions

$$(n_{z,z})_{z=0,d} = \frac{A}{K_1} \Delta n, \tag{19}$$

where $\Delta n = (n_z)_{z=0,d} - n^0$, A is the anchoring strength, and d is the sample thickness. Here $\mathbf{n}_{z=0,d}$ is the director orientation on the bounding surfaces, and $\mathbf{n}^0$ is the easy axis orientation, respectively.

Let us introduce a new vector $\overline{\mathbf{n}} = \mathbf{n}_z - \mathbf{n}^0$. The last two equations (18) and (19) can be rewritten in the form

$$\gamma_1 \overline{n}_{,t} + \frac{\alpha_2}{d} v_{z,\overline{x}} + \frac{\alpha_3}{d} v_{x,\overline{z}} + \mathcal{B}\overline{n} - \frac{K_1}{d^2} \overline{n}_{,\overline{z}\overline{z}} - \frac{K_3}{d^2} \overline{n}_{,\overline{x}\overline{x}} = 0 \tag{20}$$

and

$$(\overline{n}_{,\overline{z}})_{\overline{z}=0,1} = \frac{Ad}{K_1} \overline{n}_{\overline{z}=0,1}. \tag{21}$$

Here $\overline{x} = \frac{x}{d}$ and $\overline{z} = \frac{z}{d}$ are the dimensionless coordinates and the term $-\mathcal{B}n^0 = \text{const}$ which is not accounted for in Eq. (20). Notice that the overbars in the space variables x and z, as well as in the vector $\mathbf{n}$, will be eliminated.

The following linearized calculation derives the relationship between the growth rate s and the wavelengths q_x and q_z of an individual Fourier component of the modulation which is described by

$$\begin{aligned} n_z &= n_0 \sin(q_x x) \sin(q_z z) \exp(st), \\ v_x &= v_0 q_z \sin(q_x x) \cos(q_z z) \exp(st), \\ v_z &= -v_0 q_x \cos(q_x x) \sin(q_z z) \exp(st), \end{aligned} \tag{22}$$

where $n_0 \equiv n(t=0)$. Note that the velocities v_x and v_z on the two restricted solid surfaces have to satisfy the following boundary conditions:

$$v_z(z=0,1) = 0; \quad v_{x,z}(z=0,1) = 0. \tag{23}$$

In that case, the torque-balance equation (18) takes the form

$$\mathcal{A}_1 v_0 - \mathcal{A}_2 n_0 = 0, \tag{24}$$

where $\mathcal{A}_1 = \frac{1}{d}(\alpha_2 q_x^2 - \alpha_3 q_z^2)$ and $\mathcal{A}_2 = -\mathcal{B} - \frac{K_1}{d} q_z^2 - \frac{K_3}{d} q_x^2 - \gamma_1 s = -(\epsilon_0 \Delta\tilde{\epsilon} E^2 \cos 2\alpha + \frac{\Delta\tilde{\chi}}{\mu_0} B^2) - \frac{K_1}{d} q_z^2 - \frac{K_3}{d} q_x^2 - \gamma_1 s$. The linearized Navier-Stokes equation, Eq. (16), takes the form

$$\mathcal{A}_3 v_0 - \mathcal{A}_4 n_0 = 0, \tag{25}$$

where $\mathcal{A}_3 = \frac{1}{d^2}(\eta_1 q_z^4 + \eta_8 q_z^2 q_x^2 + \eta_2 q_x^4)$, $\mathcal{A}_4 = \frac{1}{d}(-\alpha_2 q_x^2 + \alpha_3 q_z^2) s = -\mathcal{A}_1 s$, and $\eta_8 = \eta_5 - \eta_6 - \eta_4 + \alpha_4$.

Substituting Eq. (25) into Eq. (24) and solving yields

$$s = \frac{-q_z^2 - K_{31} q_x^2 - \mathcal{B}}{1 - \frac{(\overline{\alpha}_3 q_z^2 - \overline{\alpha}_2 q_x^2)^2}{\overline{\eta}_1 q_z^4 + \overline{\eta}_2 \overline{q}_x^4 + \overline{\eta}_8 q_x^2 q_z^2}} \left[\frac{K_1}{\gamma_1 d^2}\right], \tag{26}$$

where $K_{31} = \frac{K_3}{K_1}$, $\mathcal{B} = (\frac{U}{U_c})^2 \lambda_1 \cos 2\alpha + \lambda_2$, $\lambda_1 = \epsilon_0 \Delta\tilde{\epsilon} \frac{U_c^2}{K_1}$ and $\lambda_2 = \frac{\Delta\tilde{\chi}}{\mu_0} \frac{(Bd)^2}{K_1}$ are two of the dimensionless parameters of the system, $\overline{\eta}_1 = \frac{\eta_1}{\gamma_1}, \ldots, \overline{\eta}_8 = \frac{\eta_8}{\gamma_1}$, $\overline{\alpha}_2 = \frac{\alpha_2}{\gamma_1}$, and $\overline{\alpha}_3 = \frac{\alpha_3}{\gamma_1}$ are the dimensionless viscosity coefficients, and $U_c = 200$ V.

In turn, the boundary condition can be rewritten as

$$\frac{K_1}{Ad} q_z = \tan(q_z z)_{z=0,1}. \tag{27}$$

At $z = 0$, the minimal $q_z^{\min}$ is equal to 0, whereas at $z = 1$, the minimal $q_z^{\min}$ have to be satisfied the following equation:

$$\frac{K_1}{Ad} q_z^{\min} = \tan\left(q_z^{\min}\right). \tag{28}$$

For further analysis let us consider the case of 5CB-d_2 (deuteriated 5CB in the α position of the pentyl chain) at temperature $t = 15\,^{\circ}$C and density 10^3 kg/m^3. Here we use the experimental data for elastic [20], dielectric [21], and viscous [22] coefficients for further extrapolation of these data in the lower temperature range. Notice that the nematic range for the deuteriated 5CB-d_2 is shifted to the lower temperature range ($6\,^{\circ}$C$-32\,^{\circ}$C). At temperature $t = 15\,^{\circ}$C and density 10^3 kg/m^3, the values of those coefficients were found to be elastic $K_1 = 8.7$ pN and $K_3 = 10.2$ pN, dielectric $\epsilon_{\parallel} = 19.5$ and $\epsilon_{\perp} = 8$, and rotational viscosity $\gamma_1 \sim 0.136$ Pa s and $\gamma_2 \sim -0.1507$ Pa s, respectively. In the following, we also use the measured values of the Leslie coefficients $\alpha_i (i = 1, \ldots, 6)$ [22]. The values of the voltage across the LC sample in 194.7 μm were chosen to be equal to 200 V.

All measurements of the anchoring strengths for 5CB on the glass substrates yield values of A in the range 10^{-5} to 10^{-6} J/m^2 [23]. It is allows us to calculate the root of Eq. (28). The magnitude of the dimensionless coefficient $\frac{K_1}{Ad}$ is equal to 0.044 for the value of $A = 10^{-6}$ J/m^2 (case I), and 0.0044 for the value of $A = 10^{-5}$ J/m^2 (case II), respectively. These values of $\frac{K_1}{Ad}$ provide the minimal values of the dimensionless wavelengths $q^{\min} \equiv q_z^{\min}$, which are equal to $\Delta = \pi + \delta$, where $\delta = 0.1434$ in case I and 0.01434 in case II, respectively.

Note that in the limiting case of strong anchoring, when $A \to \infty$, $\lim_{A\to\infty} \Delta = \pi$.

Taking into account that the measurements were made in the nematic phase of 5CB-d_2 using a JEOL Lambda 300 spectrometer [2,3], which has a magnetic flux density $\mathbf{B}$ of 7.05 T, the values of the dimensionless parameters λ_1 and λ_2 were estimated to be equal to 47 418 and 5486, respectively. Having obtained the values of $q_z^{\min} = \Delta$, one can calculate, by using the Eq. (26), the dimension growth rate s as a function of the dimensionless wavelength $q_x d/\pi$. Calculations of the rate s (in s^{-1}) vs $q_x d/\pi$, under influence both the electric field $U = 200$ V and the magnetic field 7.05 T, for a number of values of the angle α: 0.157 ($\sim 9^{\circ}$)[curve (1)]; 0.509 ($\sim 30^{\circ}$)[curve (2)]; 0.864 ($\sim 50^{\circ}$)[curve (3)]; 1.22 ($\sim 70^{\circ}$)[curve (4)], and 1.57 ($\sim 90^{\circ}$)[curve (5)], is shown in Fig. 7. The main result of this calculation is that the periodic response appears only for the high values of $\alpha \sim 60^{\circ}$ and higher, when the field U is strong enough to be over the threshold, and for each value of the angle $\alpha > 60^{\circ}$, there is an optimal dimensionless wavelength $q_x^{\max}$ corresponding to the fastest growth of the distortion. Our calculations also show that the character of the bounding anchoring conditions practically

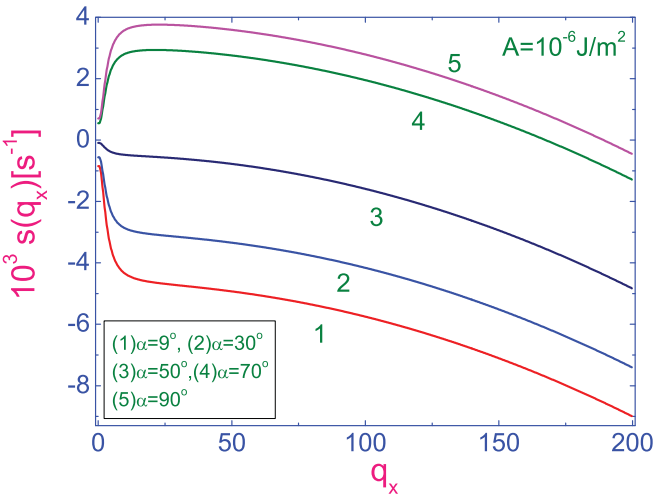

FIG. 7. (Color online) Dimension profile $s(q_x d/\pi)$ in s^{-1} vs dimensionless wavelength $q_x d/\pi$ under the influence of both the magnetic field 7.05 T and the electric field $U = 200$ V, calculated for a number of values of the angle α: 0.157 (∼9°)[curve (1)]; 0.509 (∼30°)[curve (2)]; 0.864 (∼50°)[curve (3)]; 1.22 (∼70°)[curve (4)], and 1.57 (∼90°)[curve (5)], respectively.

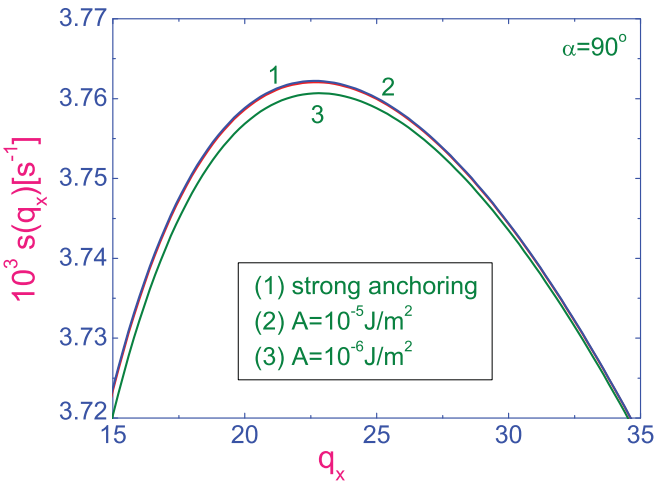

FIG. 8. (Color online) Dimension profile $s(q_x d/\pi)$ [in s^{-1}] vs dimensionless wavelength $q_x d/\pi$ under influence of both the magnetic field 7.05 T and electric field $U = 200$ V, calculated for a number of values of the anchoring strength A (in J/m^2): 10^{-6} [curve (1)]; 10^{-5} [curve (2)]; case of the strong anchoring [curve (3)], respectively. Here $\alpha \sim 90°$.

does not influence both the magnitudes of the growth rate s and the dimensionless wavelength $q_{\max} \equiv q_x^{\max}$ (see Fig. 8.) Having obtained the value of $q_{\max}$, corresponding to each value of α, one can calculate the effective viscosity

$$\gamma_{\rm eff}(\alpha) = \gamma_1\left(1 - \frac{\left(\Delta^2\overline{\alpha}_3 - \overline{\alpha}_2 q_{\max}^2\right)^2}{\Delta^4\overline{\eta}_1 + \overline{\eta}_2 q_{\max}^4 + \Delta^2\overline{\eta}_8 q_{\max}^2}\right) \quad (29)$$

as a function of the angle α.

Collected in Table I are the calculated data on the dimensionless effective viscosity $\gamma_{\rm eff}(\alpha)/\gamma_1$ as a function of the angle α, the optimal dimensionless wave vector $q_{\max}$ corresponding to the fastest growth of the distortion, and the anchoring strength A.

In the limiting case of $q_{\max} = 0$, the effective viscosity $\gamma_{\rm eff}/\gamma_1$ is equal to

$$\gamma_{\rm eff}/\gamma_1 = 1 - \frac{\overline{\alpha}_3^2}{\overline{\eta}_1}, \quad (30)$$

which agrees with the result reported in the literature [24]. When α tends to be 90°, the optimum wavelength $q_{\max}(\alpha)$, giving the fastest response, provides the lower effective viscosity $\gamma_{\rm eff}$, which is approximately five times less than one in the bulk nematic phase. Physically, this means that the periodic distortion emerging spontaneously from a homogeneous state may induce a faster response than in the uniform mode. The nonuniform rotation modes involve additional internal elastic distortions that are absent in the uniform rotation mode. This leads to a compromise that determines the wavelength of the fastest-growing periodic structure in the LC film. In turn, the large-amplitude distortions modulated in the x direction lead to the increase of the elastic energy of the conservative LC system, and as a result, it causes the decrease of the viscous contribution to the total energy of the LC system. It is obvious from Fig. 7 that there is a certain threshold value of the angle α so that the periodic distortion emerges spontaneously. That is, when α is close to a right angle [see curves (4) and (5) in Fig. 7], the value of γ_1 in Eqs. (10) and (11) should be replaced by Eq. (29). That is, a lower value of γ_1 gives the faster relaxation times, $\tau_{\rm ON}$ and $\tau_{\rm OFF}$, as observed experimentally in Fig. 6.

Thus, our theoretical analysis of the experimental results, based on the predictions of the hydrodynamic theory, including both the director motion and fluid flow, provides evidence for the appearance of spatially periodic patterns in response to a suddenly applied large electric field only at angles $\alpha > 60°$. When the values of α are less then 60°, the director reorientation can be described by the torque-balance equation for a monodomain nematic. Notice that our calculation predicts that the dynamic periodic order emerges

TABLE I. The calculated data, using Eq. (26), on the effective viscosity $\gamma_{\rm eff}(\alpha)/\gamma_1$ as a function of the angle α and the anchoring strength A.

	Strong		$A = 10^{-5} J/m^2$		$A = 10^{-6} J/m^2$	
α^o	$q_{\max}$	$\gamma_{\rm eff}/\gamma_1$	$q_{\max}$	$\gamma_{\rm eff}/\gamma_1$	$q_{\max}$	$\gamma_{\rm eff}/\gamma_1$
74	20.5	0.183	20.6	0.183	21.3	0.183
78	20.96	0.183	21.3	0.183	21.7	0.182
82	21.8	0.182	22.0	0.182	22.6	0.182
86	22.1	0.182	22.2	0.182	22.9	0.182
90	23.0	0.182	23.2	0.182	23.6	0.182

spontaneously from the homogeneous state only due to thermal fluctuations, without any initial local misalignment of the director.

It should be pointed out that the recent computer simulation predicts the existence of a new reorientation mode in confined LC film starting from an initial local misalignment of the director [6]. As a result, that mode may dominate the director reorientation in thin LC film under the influence of the large electric field applied normal to the bounding surfaces.

IV. CONCLUSION

In summary, we have investigated the peculiarities in the director relaxation observed during both the turn-on and turn-off alignment processes by using a deuterium NMR spectroscopy. The measurements show that with an increase of the angle α, $\tau_{ON}(\alpha)$ monotonically grows up to the maximum value $\tau_{ON}(\max)$ and $\tau_{OFF}(\alpha)$ keeps a constant of $\tau_{OFF}(\text{const})$. With further growth of α up to the right angle ($\alpha \sim \frac{\pi}{2}$), both $\tau_{ON}(\alpha \sim \frac{\pi}{2})$ and $\tau_{OFF}(\alpha \sim \frac{\pi}{2})$ rapidly decrease with a few milliseconds, with respect to $\tau_{ON}(\max)$ and $\tau_{OFF}(\text{const})$, respectively. These features have been investigated by accounting for the spatially periodic patterns that emerge spontaneously from the homogeneous state. It has been shown qualitatively, to understand the peculiarities observed in the experiments, that those periodic distortions cause a faster response of the director rotation on the sudden application of the large electric field than that for the monodomain mode because of a lower effective viscosity.

It would be expected that the present investigation has shed some light on the problems of the reorientation processes in nematic films confined between two plates under the presence of a large electric field directed perpendicular to the magnetic field.

ACKNOWLEDGMENTS

A.V.Z. acknowledges support from the Russian Funds for Fundamental Research (Grant No. 09-02-00010-a). A part of this work is supported financially from the HRC project (MEXT. HAITEKU 2006-2010) of Ministry of Education, Culture, Sports, Science and Technology of Japan.

[1] R. Y. Dong, *Nuclear Magnetic Resonance of Liquid Crystals*, 2nd ed. (Springer-Verlag, New York, 1997).
[2] G. R. Luckhurst, T. Miyamoto, A. Sugimura, and B. A. Timimi, J. Chem. Phys. **117**, 5899 (2002).
[3] G. R. Luckhurst, A. Sugimura, B. A. Timimi, and H. Zimmermann, Liq. Cryst. **32**, 1389 (2005).
[4] A. Sugimura and G. R. Luckhurst, in *Nuclear Magnetic Resonance Spectroscopy of Liquid Crystals*, edited by R. Y. Dong (World Scientific, Singapore, 2009), Chap. 10.
[5] M. Cifelli, D. Frezzato, G. R. Luckhurst, G. J. Moro, A. Sugimura, and C. Veracini, Liq. Cryst. **37**, 773 (2010).
[6] A. F. Martins and A. Veron, Liq. Cryst. **37**, 747 (2010).
[7] F. Lonberg, S. Fraden, A. J. Hurd, and R. E. Meyer, Phys. Rev. Lett. **52**, 1903 (1984).
[8] G. R. Luckhurst, J. Chem. Soc., Faraday Trans. 2 **84**, 961 (1988).
[9] S. M. Fan, G. R. Luckhurst, and S. J. Picken, J. Chem. Phys. **101**, 3255 (1994).
[10] J. L. Ericksen, Arch. Ration. Mech. Anal. **4**, 231 (1960).
[11] F. M. Leslie, Arch. Ration. Mech. Anal. **28**, 265 (1968).
[12] C. J. Dunn, G. R. Luckhurst, T. Miyamoto, A. Sugimura, and B. A. Timimi, Mol. Cryst. Liq. Cryst. **347**, 167 (2000).
[13] A. M. Kantola, G. R. Luckhurst, A. Sugimura, and B. A. Timimi, Mol. Cryst. Liq. Cryst. **402**, 117 (2003).
[14] D. A. Dunmur and W. H. Miller, J. Phys. (Paris):Colloq. **40**, C3-141 (1979).
[15] A. F. Martins, P. Esnault, and F. Volino, Phys. Rev. Lett. **57**, 1745 (1986).
[16] Antonino Polimeno, Laura Orian, Assis F. Martins, and Alexandre E. Gomes, Phys. Rev. E **62**, 2288 (2000).
[17] Assis F. Martins, Alexandre E. Gomes, Antonino Polimeno, and Laura Orian, Phys. Rev. E **62**, 2301 (2000).
[18] G. R. Luckhurst, T. Miyamoto, A. Sugimura, B. A. Timimi, and H. Zimmermann, J. Chem. Phys. **121**, 1928 (2004).
[19] A. Sugimura, A. A. Vakulenko, and A. V. Zakharov, Physics Procedia **14**, 102 (2011).
[20] N. V. Madhusudana and R. P. Pratibha, Mol. Cryst. Liq. Cryst. **89**, 249 (1982).
[21] A. V. Zakharov and A. Maliniak, Eur. Phys. J. E **4**, 435 (2001).
[22] A. G. Chmielewski, Mol. Cryst. Liq. Cryst. **132**, 339 (1986).
[23] L. M. Blinov, A. Yu. Kabaenkov, and A. A. Sonin, Liq. Cryst. **5**, 645 (1989).
[24] E. Guyon, R. B. Meyer, and J. Salan, Mol. Cryst. Liq. Cryst. **54**, 261 (1979).